Electron collisions with nitrogen trifluoride (NF_3) molecules

Czesław Szmytkowski,* Alicja Domaracka, Paweł Możejko,† Elżbieta Ptasińska-Denga, Łukasz Kłosowski, Michał Piotrowicz, and Grzegorz Kasperski

Atomic Physics Group, Faculty of Applied Physics and Mathematics, Gdańsk University of Technology, ul. G. Narutowicza 11/12, 80-952 Gdańsk, Poland

(Received 9 June 2004; published 22 September 2004)

Absolute total cross sections (TCS's) for 0.5–370-eV electrons scattered by nitrogen trifluoride (NF_3) molecules have been measured using a linear transmission method under single collision conditions. It was found that the TCS energy function for NF_3 is dominated with two pronounced enhancements: one resonantlike centered between 2 and 3 eV with the maximum value of 28×10^{-20} m^2 followed with a minimum at around 7–12 eV($\sim17\times10^{-20}$ m^2), and the second much broader enhancement located around 40 eV (19×10^{-20} m^2 in the maximum). The low-energy enhancement is superimposed with some weak features located near 1.8, 2.2, and 2.8 eV. The integral elastic cross section has been calculated at intermediate energies using an independent atom method with a static plus polarization model potential. The cross section for ionization has been computed as well using the binary-encounter-Bethe approach. The sum of calculated cross sections reasonably reproduces the intermediate-energy experimental TCS, with respect to the shape and value. The TCS for NF_3 is also compared with the TCS for ammonia (NH_3) which was supplementary measured and the effect of substitution of fluorine atoms for hydrogen (perfluorination effect) is demonstrated and discussed.

DOI: 10.1103/PhysRevA.70.032707 PACS number(s): 34.80.Bm, 34.80.Gs

I. INTRODUCTION

New concepts and advancement of many present-day technologies need the basic knowledge of the wide range of electron-molecule processes and comprehensive information on behavior of electrons in low-temperature plasma [1]. Nitrogen trifluoride (NF_3), first synthesised over 80 years ago [2], is widely used as an efficient fluorine source for the production of very large-scale integrated electronics [3,4], and in rare gas-halide excimer laser systems [5]. It is also used for synthesis of fluorine containing compounds [6]. What is important, in the absence of strong activation, NF_3 appears to be a quite inert and environmental friendly compound [7].

Experiment using electrons for the study of NF_3 structure was carried out not earlier than in the half of past century [8]. Further experimental studies were performed on variety of electron-stimulated processes for this molecule: direct and/or dissociative ionization [9–12], the negative ion formation [9,13–17], the dissociation involving emission [18], the elastic scattering and vibrational excitation [19]. Behavior of electrons in gaseous NF_3-containing media [5,20–26], as well as electron-stimulated surface chemistry of NF_3 [27], were also investigated. In spite of such wealth of experimental works concerning electron-NF_3 interaction only few give the intensity of studied processes in absolute scale. From the computational side, the e^--NF_3 scattering has come to attention quite recently [28–31].

The main goal of the present paper is to provide accurate absolute total cross section (TCS) data for electron scattering from the NF_3 molecule over a wide energy range. These results should stimulate further experiments and more refined theoretical developments.

In order to investigate how the electron-scattering cross-section energy dependence changes when all hydrogen atoms in a molecule are replaced by fluorine, we have compared the TCS results for NF_3 with those for its hydrogenated counterpart, NH_3. There are already some TCS data for NH_3 available from various laboratories, the absolute [32–36] and normalized [37] ones. However, results from different laboratories differ from each other as to the magnitude (cf. Ref. [38]) in the overlapping energy range; the most serious deviations arise in the TCS maximum resonant region (up to 25%), around 10 eV, and at high energies (to 35%). For proper comparison it is more appropriate to have data from the same laboratory. For this purpose the TCS for NH_3 was also measured in the present work.

For a better understanding of the intermediate energy enhancement, observed in TCS energy functions for fully fluorinated compounds, we have also computed the elastic cross section at intermediate energies and the ionization cross section for the e^--NF_3 scattering; their sum—calculated "total" cross section—is used for comparison with the present experimental TCS results.

II. METHODS AND PROCEDURES

A. Experiment

The TCS for electron scattering has been measured employing the transmission method [39] in a linear configuration. The apparatus and measuring procedure is similar to that extensively used in our previous TCS experiments. Since a detailed description has been given previously [40,41], only a brief summary is presented here. The electron beam of a given energy E is formed by an electron gun

*Electronic address: czsz@mif.pg.gda.pl

†Present address: Department of Nuclear Medicine and Radiobiology, University of Sherbrooke, Canada.

 ©2004 The American Physical Society

followed by an energy dispersing cylindrical electrostatic monochromator and directed into the interaction cell by an electron zoom lens system. The electrons which pass the scattering volume are energy discriminated by a retarding-field element and eventually detected by a Faraday cup. When target molecules are admitted into the scattering cell, the transmitted electrons suffer scattering what reflects in the attenuation of a recorded electron current.

To determine the TCS value $Q(E)$ we used the Bouguer–de Beer–Lambert (BBL) attenuation formula:

$$Q(E) = \frac{k}{pl}\sqrt{T_m T_g}\,\ln\frac{I_0(E)}{I_g(E)},$$

where k is the Boltzmann constant, l is the effective path length of the interaction region in the target, p is the pressure of the investigated target gas, T_m is the temperature of the manometer head (322 K), T_g is the temperature of the scattering cell, and I_p and I_0 are, respectively, the intensities of the transmitted electron currents in the presence and absence of the target gas in the scattering cell; the formula takes into account the thermal transpiration effect [42]. The electron energy scale is calibrated by the well-known standard—the 2.3-eV oscillatory resonant structure in N_2. The spectrometer works with a typical incident electron current of 0.1–100 pA, and energy resolution of about 80 meV (full width at half maximum).

The measurements were carried out for a given energy in series of runs. Within limits of statistical uncertainties, the results obtained in different series were independent of applied sample pressures (80–260 mPa) and the electron-beam controlling parameters. An averaging procedure with weights depending on the statistical uncertainty was applied to derive the final total cross section at a particular energy. The scatter of TCS results (one standard deviation of the weighted mean value) reaches about 1.5% below 1 eV while being well below 1% at intermediate energies.

With the use of present method, the determination of absolute TCS values is possible because all quantities in the BBL formula can be directly measured or determined. However, even if the TCS measurements by the transmission method are performed very carefully, the results are charged with systematic uncertainties inherently connected with the method itself. The BBL attenuation formula does not take into consideration two important effects: (i) the most troublesome one, which systematically lowers measured TCS, is related to the fact that apart of unscattered electrons detected are electrons which undergo the elastic forward scattering through small angles; the retarding-field filter prevents only the electrons scattered inelastically with energy losses higher than 100 meV to be detected. The forward scattering increases with the increase of the electric dipole moment of scatterer and with energy. Uncertainties related to the imperfect discrimination of electrons scattered into small forward angles can be estimated if angular distribution for elastic electron scattering at each energy is available, especially at close to zero angles. Based on the differential elastic cross-section data [19,31] we estimated that the amount by which the present TCS may be too low due to elastic forward-scattering should not exceed 1% at 100 eV decreasing steadily down to 0.2% in the resonance region. At the highest energies used in the present experiment (370 eV) anticipated uncertainty amounts about 2–3%; (ii) another inevitable problem is connected with the end effects at the entrance and exit apertures of the scattering cell. The target-gas flow through the chamber orifices causes the inhomogeneous pressure distribution inside the scattering cell. On the other hand, the presence of the effusing sample particles outside the cell does not allow us to determine accurately the real path length of electrons within the target region. In consequence, the uncertainty appears in evaluation of the factor pl in the denominator of BBL formula. Estimations based on the calculations of Nelson and Colgate [43] show that for the present geometry the end effect contributes to the uncertainty of TCS less than 1% when the factor pl is replaced with the product $p_m L$, where p_m is the sample pressure as read by the mks manometer head and L(=30.5 mm) is the distance between entrance and exit apertures of the reaction cell. Sum of the other possible systematic errors, encountered in the measurements of the electron beam current and of the target pressure, have been estimated to be less than 2%. The NF_3 sample with a stated purity 99.99% obtained from ABCR GmbH and NH_3 (99.96%) from Merck were used directly from supplied cylinders.

B. Computation

The theoretical approaches and computational procedures used in the present calculations are essentially the same as employed and described in our earlier studies [44], so only a brief summary follows. The elastic cross section for electron collisions with NF_3 molecules is calculated with the independent atom method (IAM) [45], in which the integral elastic cross section for electron scattering by a molecule is given by

$$\sigma(E) = \frac{4\pi}{k}\sum_{i=1}^{N}\mathrm{Im} f_i(\theta = 0, k) = \sum_{i=1}^{N}\sigma_i^A(E),$$

where E is an energy of the incident electron, $f_i(\theta, k)$ is the scattering amplitude due to the ith atom of the molecule, θ is the scattering angle, and $k = \sqrt{2E}$ is the wave number of the incident electron. The atomic elastic cross section of the ith atom of the target molecule, $\sigma_i^A(E)$, is derived according to

$$\sigma^A = \frac{4\pi}{k^2}\left(\sum_{l=0}^{l_{max}}(2l+1)\sin^2\delta_l + \sum_{l=l_{max}}^{\infty}(2l+1)\sin^2\delta_l^{(B)}\right).$$

To obtain phase shifts δ_l, partial wave analysis is employed and the radial Schrödinger equation,

$$\left[\frac{d^2}{dr^2} - \frac{l(l+1)}{r^2} - 2[V_{\mathrm{stat}}(r) + V_{\mathrm{polar}}(r)] + k^2\right]u_l(r) = 0,$$

is solved numerically under the boundary conditions

$$u_l(0) = 0, \quad u_l(r) \overset{r\to\infty}{\sim} a_l\hat{j}_l(kr) - b_l\hat{n}_l(kr),$$

where $\hat{j}_l(kr)$ and $\hat{n}_l(kr)$ are the Riccati-Bessel and Riccati-Neumann functions, respectively. The electron-atom interac-

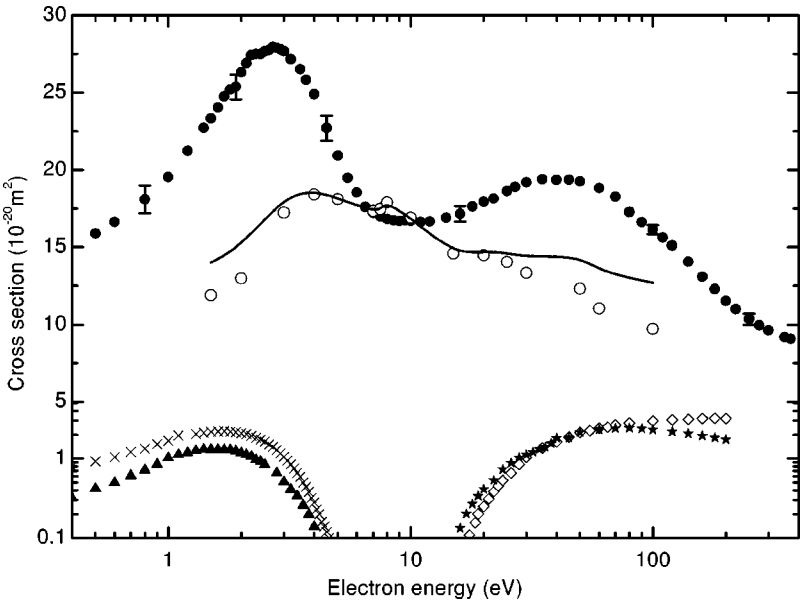

FIG. 1. Experimental cross sections for e^--NF_3 scattering: full circles, present TCS, error bars represent overall (systematic plus statistical) uncertainties; open circles, elastic [19]; full stars, total ionization [11]; open diamonds, total ionization [12]; full triangles, dissociative attachment [15]; crosses, dissociative attachment [17]. Full line represents experimental total cross section obtained as the sum of the elastic [19], the ionization [12], and the attachment [17] cross sections. Note: the cross-section scale is the log scale below 5.

tion is represented by the static $V_{\text{stat}}(r)$ [46] and polarization $V_{\text{polar}}(r)$ [47] potentials. The phase shifts δ_l are connected with asymptotic form of the wave function $u_l(r)$, by

$$\tan\ \delta_l = \frac{b_l}{a_l}.$$

In the present calculations the exact phase shifts are calculated for l up to $l_{max}=50$ while those remaining, $\delta_l^{(B)}$, are included through the Born approximation.

The electron-impact ionization cross section is obtained within the binary-encounter-Bethe (BEB) formalism [48] in which the electron-impact ionization cross section per molecular orbital is given by

$$\sigma_{BEB} = \frac{S}{t+u+1}\left[\frac{\ln t}{2}\left(1-\frac{1}{t^2}\right)+1-\frac{1}{t}-\frac{\ln t}{t+1}\right],$$

where $u=U/B$, $t=T/B$, $S=4\pi a_0^2 NR^2/B^2$, $a_0=0.5292$ Å, $R=13.61$ eV, and T is the energy of incident electron. The electron binding energy B, kinetic energy of the orbital U, and orbital occupation number N, are calculated for the ground state of the investigated molecule with the Hartree-Fock method using the GAMESS code [49], and GAUSSIAN 6-311G basis set. Because energies of the highest occupied molecular orbitals (HOMO) obtained this way can usually differ from experimental ones, we performed also outer valence Green function calculations of correlated electron affinities and ionization potentials [50,51] using the GAUSSIAN code [52]. Finally, the experimental values [53] of the first ionization potential have been inserted in the calculation, instead those obtained theoretically, to fix the threshold behavior of the ionization cross section at the experimental value. The total ionization cross section is obtained as the sum of σ_{BEB} for all molecular orbitals.

III. RESULTS AND DISCUSSION

In this section we present our electron scattering TCS for the NF_3 and NH_3 molecules measured in the transmission experiment over energy range from 0.5 (0.6) to 370 eV. We also make some remarks on the comparison of the obtained TCS for NF_3 with the sum of available experimental partial cross sections. Same comparison of the TCS is also made with the sum of calculated elastic and ionization cross sections for this molecule. Later, comparison of the present TCS for NF_3 with our data for NH_3 is made and the perfluorination effect is indicated and discussed.

A. Nitrogen trifluoride, NF_3

The variation of the absolute total electron-scattering cross section for NF_3 with an electron energy is shown in Fig. 1 together with other available experimental cross sections: the elastic integral obtained by Boesten *et al.* [19], for electron attachment by Chantry [15] and Nandi *et al.* [17], and the total ionization taken by Tarnovsky *et al.* [11] and Haaland *et al.* [12]. The numerical TCS values from the present experiments are listed in Table I.

Figure 2 confronts the present TCS with theoretical cross sections: the integral elastic calculated by Joucoski and Bettega [31], the ionization by Deutch *et al.* [29], and with the present elastic and ionization cross-section calculations.

As neither experimental nor theoretical TCS data are available in the literature, for further discussion we used: (i) the sum of experimental electron attachment [17], the elastic [19] and ionization [12] cross sections; i.e., the experimental "total" cross section (Fig. 1) and, (ii) the sum of computed integral elastic cross sections from Ref. [31] and the present one, both spliced at 60 eV, and the present ionization cross section; i.e., calculated total cross section (Fig. 2). With respect to the shape, both total cross sections, experimental as well as theoretical, agree resonably well with the present TCS results in the overlapping energy range. However, the low-energy maximum in the experimental total cross section (Fig. 1), appears to be rather weakly marked and distinctly lower (by 30–40%) than the maximum in our TCS and shifted by 1 eV to higher energy (near 4 eV). The agreement

TABLE I. Absolute electron-scattering total cross sections for NH_3 and NF_3 molecules in 10^{-20} m^2.

E	TCS		E	TCS	
(eV)	NH_3	NF_3	(eV)	NH_3	NF_3
0.5		15.9	9	23.1	16.7
0.6	17.6	16.6	9.5	23.4	16.7
0.7	16.7		10	23.3	16.7
0.8	15.8	18.1	11	22.9	16.6
1.0	14.4	19.6	12	21.7	16.7
1.2	13.3	21.2	14		16.9
1.4		22.7	15	19.6	
1.5	11.9	23.3	16		17.2
1.6		24.0	17	18.5	
1.7		24.8	18		17.6
1.8		25.2	20	17.5	17.9
1.9		25.4	22	16.8	18.2
2.0	10.9	26.3	25	15.8	18.6
2.1		26.9	27	15.1	18.9
2.2		27.4	30	14.4	19.2
2.3		27.5	35	13.5	19.4
2.4		27.5	40	12.8	19.4
2.5	10.7	27.7	45	12.3	19.4
2.6		27.8	50	11.6	19.3
2.7		28.0	60	10.7	18.8
2.8		27.9	70	10.1	18.3
2.9		27.8	80	9.75	17.3
3.0	11.0	27.7	90	9.24	16.6
3.2		27.2	100	8.88	16.1
3.5	11.9	26.5	110	8.27	15.6
3.7		25.8	120	7.85	15.1
4.0	12.5	24.9	140	7.12	14.1
4.5	14.3	22.7	160	6.62	13.1
5.0	15.9	20.9	180	6.19	12.3
5.5	16.5	19.5	200	5.81	11.5
6.0	17.7	18.5	220	5.49	11.0
6.5	19.1	17.6	250	4.93	10.4
7.0	20.3	17.2	275	4.59	9.94
7.5	21.1	17.0	300	4.23	9.63
8.0	22.0	16.8	350	3.92	9.18
8.5	22.6	16.7	370	3.64	9.07

between the TCS and experimental total cross section significantly improves in the range 6–12 eV, worsening again up to about 20% around the second maximum at 40 eV; it is worth noting that the compared cross sections still lie within combined experimental uncertainties. On the other hand, calculated total cross section, elastic plus ionization, has the resonant maximum shifted up to 7 eV (Fig. 2). At intermediate energies, the sum of calculated cross sections is in satisfactory accordance with our experimental TCS, to within 10%.

The present TCS energy dependence has two distinct features:

(i) the first one is a pronounced enhancement, spanned from the lowest energy used (0.5 eV) up to about 10 eV, with rather flat maximum of 28×10^{-20} m^2 between 2.2 and 3 eV. On this enhancement one can discerne some weak structures located at 1.8, 2.3, and 2.8 eV; though they are comparable in the magnitude to random fluctuations in single runs, they are well repetitive. The shape of the TCS curve around 2.5 eV suggests that the low-energy enhancement might be resonant in origin, that is, the electron scattering in this energy region goes, apart of direct processes, also through temporary attaching of the probe electron to molecule for a resident time longer comparing to the transit time of an electron through a region of molecular dimension. The short-lived anion decays via autodetachment of the extra electron to the parent molecule in its vibrational states or decomposes into a variety of negative and neutral fragments. The flateness and width of the TCS maximum (about 3 eV at half maximum) suggest the possibility of more than one unresolved capture processes in this energy range. The formation of only one shape resonance around 3 eV, assigned to orbital of E symmetry, has been deduced by Boesten *et al.* [19] from their experimental vibrational excitation functions. Earlier, Rescigno [30] has noticed the presence of a broad shape resonance around 5.5 eV in the calculated momentum-transfer cross section and suggested that this resonant state could be also responsible for the observed dissociation of molecule. The dissociative electron attachment channel appears to be very effective for NF_3 molecule; the total attachment cross section peaks around 1.7 eV (see Fig. 1) with the value nearly 2.2×10^{-20} m^2 [17]. More detailed analysis of dissociative products (F^-, F_2^-, and NF_2^-) [16] shows that in this energy range two resonant states are possible: one in the electronic ground state—centered at 1.8 eV, and the other, electronically excited—near 2.2 eV. Notice, that at the same energies two lowest features of the present TCS are located. Further evidence for the formation of two closely spaced low-energy shape resonances (assigned to the E and A_1 orbitals) arises from elastic calculations of Joucoski and Bettega [31]. The location of these resonances is, however, shifted to much higher energy ($\sim$7 eV) due to neglecting polarization effects.

As the elastic integral cross section measured by Boesten *et al.* [19] is in the region of the 2–3-eV resonance distinctly lower (by about 35%) than the present TCS (Fig. 1), one might attribute this difference to a considerable role of vibrationally inelastic processes. The estimated contribution from the most effective vibrational channels appears to be close to 10% [19] of that elastic. The observed deficiency in the magnitude of the cross section may also result simply from relatively high uncertainty ($\sim$30%) of the Boesten normalization procedure.

(ii) starting from about 10 eV, where the TCS has its minimum (17×10^{-20} m^2), the second very broad enhancement extends nearly to more than 100 eV peaking between 30 and 50 eV with the value of 19×10^{-20} m^2. This enhancement seems to be related mostly to elastic scattering [31], although with noticeable contribution from other allowed channels like ionization [11,12] and dissociative excitation [18,30]. An argument for such supposition comes from the sum of experimental elastic and ionization cross sections that

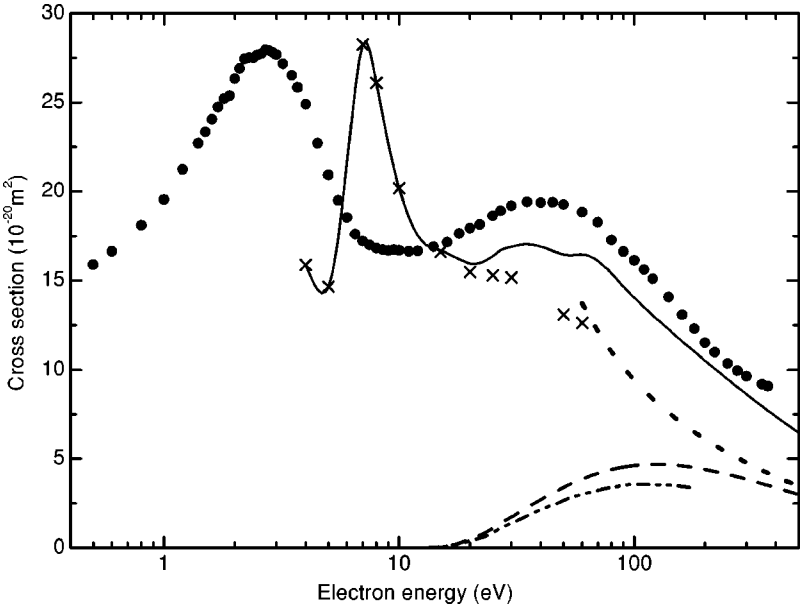

FIG. 2. Comparison of the TCS for e^--NF_3 scattering (full circles, present) with computed cross sections: crosses, integral elastic [31]; dotted line, present elastic; dashed-dot-dot line, ionization [29]; dashed line, present ionization; full line, sum of elastic (below 60 eV from Ref. [31], beyond 60 eV present results) and ionization (present) cross sections.

has a weak shoulder in the region of 20–60 eV while its magnitude is consistent with the TCS in the limit of combined uncertainties. Even better confirmation for the ground of the 20–100-eV TCS enhancement gives the sum of calculated elastic and ionization cross sections which has quite remarkable hump located in the same energy range (Fig. 2). The descending part of the TCS, above 100 eV, can be approximated with the function $Q \sim E^{-0.5}$, that means the TCS is proportional to the time the incoming electron needs to cross the molecular dimension.

It is interesting that around 8–10 eV, where perfluorides usually have their maximum, for NF_3 only very weak feature may be discernible. It is also worth noting two weak structures superimposed onto this broad enhancement: around 12 eV some weak knee in the TCS curve is visible, that might be associated with the electronic excitation of NF_3 molecule [30], while very broad structure spanned between 110 and 180 eV may reflect the ionization cross section maximum observed in this energy range [12,29].

B. Perfluorination effect

The changes in electron scattering cross sections caused by replacing of hydrogen atoms in molecule with fluorine are already known since systematic studies of cross sections have been performed for polyatomic perfluorinated compounds and their perhydrogenated homologues (see, Refs. [54] and [55], and the references therein). It was found that differences between TCS's for fully fluorinated and hydrogenated compounds (e.g., hydrocarbons and respective fluorocarbons) are characterized by some regularities (fluorination effects) [54,56].

To further examine how perfluorination affects the TCS and if the observed earlier regularities are also valid for more

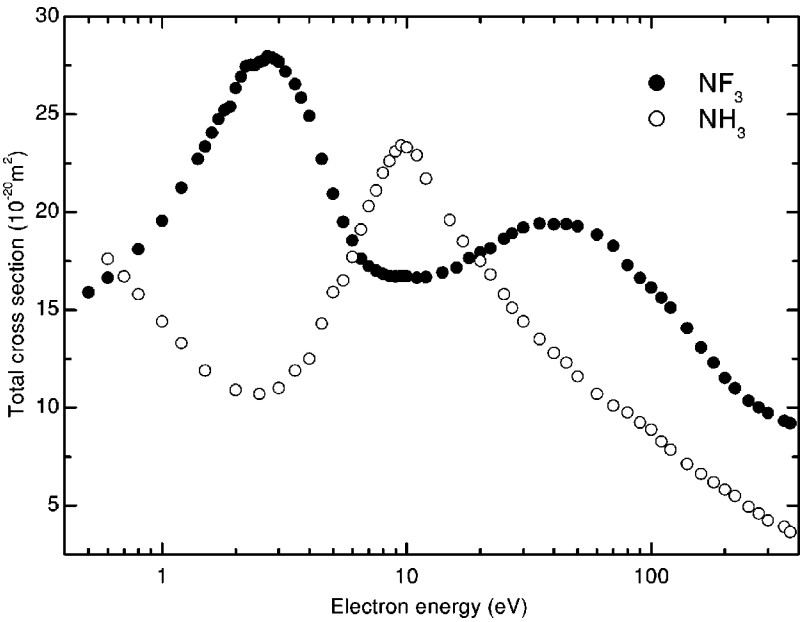

FIG. 3. Illustration of perfluorination effect. Present experimental total cross sections: full circles, NF_3; open circles, NH_3.

TABLE II. Molecular electric dipole moments μ, electric dipole polarizabilities α, ionization potentials IP, and the gas-kinetic cross sections σ.

Molecule	μ (D)	α (10^{-30} m^3)	IP (eV)	σ (10^{-20} m^2)
NH_3	1.471	2.1–2.81	10.16	7.49
NF_3	0.235	3.62	13.00	9.67

simple compounds we compared the present TCS for the e^--NF_3 scattering with measurements for NH_3. Though some TCS's for NH_3 have already been reported [32–37], the problem arises as to which of the TCS sets should be selected for comparison with NF_3 as the results obtained with different techniques differ substantially in the magnitude (see Ref. [38]). In general, results obtained with the techniques employing the magnetic field for selection and/or guidance of the electron beam [32,34,37] are lower than those taken with electrostatic devices only [33,35,36]. Around 10 eV, close to the TCS maximum, differences reach even 25%. Because such systematic experimental factors might strongly alter conclusions, we measured TSC also for NH_3 to reduce this problem. The NH_3 data we used for comparison are below 1 eV and beyond 80 eV our new TCS results, while between 1 and 80 eV, where energies used in old and new experiments overlap, the data are weighted mean values from our previous [33] and new measurements (the numerical data are given in Table I). Figure 3 shows the energy dependence of the present experimental TCS for NF_3 and that for NH_3.

It is clearly evident that the substitution of fluorine atoms for hydrogen in the investigated molecule changes drastically the magnitude and shape of the TCS over the entire energy range studied. Regarding the shape, for energies below 50 eV both TCS's behave antypathetic: while e^--NF_3 function descends with the energy decrease that for the NF_3 increases and vice versa. Below 6 eV the TCS for NF_3 remarkably exceeds that for NH_3. From 6 eV up to 18 eV the TCS for NH_3 becomes distinctly higher while above 20 eV the interrelation of TCS's changes and TCS for NF_3 is again much higher. This behavior confirmes our earlier findings [57,58]. As the differences of TCS's at intermediate energies can be simply explained with larger geometrical size of perfluorinated targets in comparison to hydrides, at energies below 20–30 eV the reason of differences seems to be more subtle and must be rather related to internal structure of compared molecules. At 0.7 eV the TCS curves for NH_3 and NF_3 intersect again—the effect we did not observe before. Such behavior may be related to high ratio of electric dipole moments of compared molecules (see Table II); for other pairs of molecules studied so far the dipole moments of perfluorines and their hydrogen containing homologes did not differ so much. It is also interesting to notice that the experimental TCS for NH_3 equals gas-collision cross section near 200 eV while such accord for NF_3 occurs not before 300 eV; same relation holds for other perfluorinated and perhydrogenated analogs [57,58].

IV. SUMMARY

In this work we reported the absolute total electron-scattering cross sections for NF_3 and for NH_3 molecules measured in a linear transmission experiment from 0.5 to 370 eV. The TCS energy dependence for NF_3 shows two distinct enhancements. Much more pronounced enhancement—resonant in character—is centered between 2.2 and 3 eV and superimposed with weak features located at 1.8, 2.2, and 2.8 eV. The second enhancement is very broad with the maximum placed within 30–50 eV. Comparison the the TCS data for NF_3 with the sum of existing experimental partial cross sections and with the sum of calculated cross sections suggests the source of the intermediate energy enhancement. Present data for ammonia are in good agreement with previous results according to the shape of TCS energy function but are generally higher, especially around the maximum near 9.5 eV. A comparison of the TCS's for NF_3 with that for NH_3 indicates a distinct perfluorination effect over the entire energy range studied.

The current level of understanding e^--NF_3 scattering is still not satisfactory and to explain all observed features of TCS for NF_3 and quantify the scattering process, more detailed theoretical studies as well as additional experimental information on various scattering channels are required.

ACKNOWLEDGMENTS

The authors acknowledge partial support from the KBN and from MENiS.

[1] L. G. Christophorou and J. K. Olthoff, *Fundamental Electron Interactions with Plasma Processing Gases* (Kluwer/Plenum, New York, 2004).
[2] O. Ruff, J. Fischer, and F. Luft, Z. Anorg. Allg. Chem. **172**, 417 (1928).
[3] V. M. Donnelly, D. L. Flamm, W. C. Dautremont-Smith, and D. J. Werder, J. Appl. Phys. **55**, 242 (1984).
[4] J. J. Wang, E. S. Lambers, S. J. Pearton, M. Ostling, C.-M. Zetterling, J. M. Grow, and F. Ren, Solid-State Electron. **42**, 743 (1998).
[5] M. J. Shaw and J. D. C. Jones, Appl. Phys. **14**, 393 (1977).
[6] T. Takagi, M. Tamura, M. Shibakami, H.-D. Quan, and A. Sekiya, J. Fluorine Chem. **101**, 15 (2000); **105**, 45 (2000).
[7] L. T. Molina, P. J. Wooldridge, and M. J. Molina, Geophys. Res. Lett. **22**, 1873 (1995).
[8] V. Schomaker and C.-S. Lu, J. Am. Chem. Soc. **72**, 1182 (1950).
[9] R. M. Reese and V. H. Dibeler, J. Chem. Phys. **24**, 1175 (1956).
[10] S. A. Rogers, P. J. Miller, and S. R. Leone, Chem. Phys. Lett. **166**, 137 (1990).
[11] V. Tarnovsky, A. Levin, K. Becker, R. Basner, and M. Schmidt, Int. J. Mass Spectrom. Ion Processes **133**, 175 (1994).

[12] P. D. Haaland, C. Q. Jiao, and A. Garscadden, Chem. Phys. Lett. **340**, 479 (2001).
[13] J. C. J. Thynne, J. Phys. Chem. **73**, 1586 (1969).
[14] P. W. Harland and J. L. Franklin, J. Chem. Phys. **61**, 1621 (1974).
[15] P. J. Chantry, ARPA Order No. 3342, Final Techn. Rep. (1978).
[16] N. Ruckhaberle, L. Lehmann, S. Matejcik, and E. Illenberger, J. Phys. Chem. A **101**, 9942 (1997).
[17] D. Nandi, S. A. Rangwala, S. V. K. Kumar, and E. Krishnakumar, Int. J. Mass Spectrom. Ion Processes **205**, 111 (2001).
[18] Z. J. Jabbour, K. A. Banks, K. E. Martus, and K. Becker, J. Chem. Phys. **88**, 4252 (1988).
[19] L. Boesten, Y. Tachibana, Y. Nakano, T. Shinohara, H. Tanaka, and M. A. Dillon, J. Phys. B **29**, 5475 (1996).
[20] K. G. Mothes, E. Schultes, and R. N. Schindler, J. Phys. Chem. **76**, 3758 (1972).
[21] G. D. Sides and T. O. Tiernan, J. Chem. Phys. **67**, 2382 (1977).
[22] K. J. Nygaard, H. L. Brooks, and S. R. Hunter, IEEE J. Quantum Electron. **QE-15**, 1216 (1979).
[23] D. W. Trainor and J. H. Jacob, Appl. Phys. Lett. **35**, 920 (1979).
[24] V. K. Lakdawala and J. L. Moruzzi, J. Phys. D **13**, 377 (1980).
[25] T. M. Miller, J. F. Friedman, A. E. S. Miller, and J. F. Paulson, Int. J. Mass Spectrom. Ion Processes **149/150**, 111 (1995).
[26] T. H. Hayashi, A. Kono, and T. Goto, Jpn. J. Appl. Phys., Part 1 **36**, 4651 (1997).
[27] K. H. Junker and J. M. White, Surf. Sci. **382**, 67 (1997).
[28] S. Ushiroda, S. Kajita, and Y. Kondo, J. Phys. D **23**, 47 (1990).
[29] H. Deutsch, T. D. Märk, V. Tarnovsky, K. Becker, C. Cornelissen, L. Cespiva, and V. Bonacic-Koutecky, Int. J. Mass Spectrom. Ion Processes **137**, 77 (1994).
[30] T. N. Rescigno, Phys. Rev. A **52**, 329 (1995).
[31] E. Joucoski and M. H. F. Bettega, J. Phys. B **35**, 783 (2002).
[32] E. Brüche, Ann. Phys. (Leipzig) **1**, 93 (1929).
[33] Cz. Szmytkowski, K. Maciąg, G. Karwasz, and D. Filipović, J. Phys. B **22**, 525 (1989).
[34] A. Zecca, G. P. Karwasz, and R. S. Brusa, Phys. Rev. A **45**, 2777 (1992).
[35] G. García and F. Manero, J. Phys. B **29**, 4017 (1996).
[36] W. M. Ariyasinghe, T. Wijeratne, and P. Palihawadana, Nucl. Instrum. Methods Phys. Res. B **217**, 389 (2004).
[37] O. Sueoka, S. Mori, and Y. Katayama, J. Phys. B **20**, 3237 (1987).
[38] G. P. Karwasz, R. S. Brusa, and A. Zecca, Riv. Nuovo Cimento **24**, 1 (2001).
[39] B. Bederson and L. J. Kieffer, Rev. Mod. Phys. **43**, 601 (1971).
[40] Cz. Szmytkowski, P. Możejko, and G. Kasperski, J. Phys. B **31**, 3917 (1998).
[41] Cz. Szmytkowski and P. Możejko, Vacuum **63**, 549 (2001).
[42] M. Knudsen, Ann. Phys. (Leipzig) **31**, 205 (1910).
[43] R. N. Nelson and S. O. Colgate, Phys. Rev. A **8**, 3045 (1973).
[44] P. Możejko, B. Żywicka-Możejko, and Cz. Szmytkowski, Nucl. Instrum. Methods Phys. Res. B **196**, 245 (2002).
[45] N. F. Mott and H. S. W. Massey, *The Theory of Atomic Collisions* (Oxford University Press, Oxford, 1965).
[46] F. Salvat, J. D. Martinez, R. Mayol, and J. Parellada, Phys. Rev. A **36**, 467 (1987).
[47] N. T. Padial and D. W. Norcross, Phys. Rev. A **29**, 1742 (1984).
[48] Y.-K. Kim and M. E. Rudd, Phys. Rev. A **50**, 3954 (1994).
[49] M. W. Schmidt, K. K. Baldridge, J. A. Boatz, S. T. Elbert, M. S. Gordon, J. H. Jensen, S. Koseki, N. Matsunaga, K. A. Nguyen, S. Su, T. L. Windusn, M. Dupuis, and J. A. Montgomery, Jr., J. Comput. Chem. **14**, 1347 (1993).
[50] L. S. Cederbaum, J. Phys. B **8**, 290 (1975).
[51] V. G. Zakrzewski and W. von Niessen, J. Comput. Chem. **14**, 13 (1994).
[52] M. J. Frisch *et al.*, Gaussian 98, revision A.11.2, Gaussian Inc., Pittsburgh, PA.
[53] *CRC Handbook of Chemistry and Physics*, 76th Edition, edited by D. L. Lide (CRC Press, Boca Raton, FL, 1995).
[54] Cz. Szmytkowski and E. Ptasińska-Denga, Vacuum **63**, 545 (2001).
[55] O. Sueoka, C. Makochekanwa, and H. Kawate, Nucl. Instrum. Methods Phys. Res. B **192**, 206 (2002).
[56] H. Tanaka, T. Masai, M. Kimura, T. Nishimura, and Y. Itikawa, Phys. Rev. A **56**, R3338 (1997).
[57] Cz. Szmytkowski and S. Kwitnewski, J. Phys. B **35**, 2613 (2002); **36**, 2129 (2003); **36**, 4865 (2003).
[58] Cz. Szmytkowski, S. Kwitnewski, and E. Ptasińska-Denga, Phys. Rev. A **68**, 032715 (2003).